 

PACS numbers: 79.20.Ws; 52.38.Dx; 42.65.Re; 33.80.Wz
DOI: 10.1070/QE2012v042n09ABEH014960

# Numerical investigation of the effect of the temporal pulse shape on modification of fused silica by femtosecond pulses

A.V. Dostovalov, A.A. Wolf, S.A. Babin, M.V. Dubov, V.K. Mezentsev

*Abstract.* **We report the results of numerical studies of the impact of asymmetric femtosecond pulses focused in the bulk of the material on the femtosecond modification of fused silica. It is shown that such pulses lead to localisation of absorption in the process of femtosecond modification and to a decrease in the threshold energy of modification. It is found that the optimal asymmetry parameters for reaching the maximum plasma density in the focusing region depend on the pulse energy: at an initial energy of about 100 nJ, it is preferable to use pulses with positive TOD; however, when the energy is increased, it is preferable to use pulses with negative TOD. This is explained by differences in the dynamics of the processes of absorption of energy of a pulse propagating in the material.**

***Keywords:*** *femtosecond modification, laser micromachining, refractive index, nonlinear Schrödinger equation.*

## 5. Introduction

Femtosecond laser technologies making it possible to produce high-energy ultrashort pulses are increasingly used in laser processing of materials, called femtosecond micromachining. In comparison with other well-developed methods of laser processing (cutting, ablation, polymerisation, etc.), the key advantage of femtosecond micromachining is the possibility of a local change in the refractive index of nonphotosensitive transparent materials, which allows one to create elements of integrated optics, i.e., three-dimensional waveguide structures in insulators (mainly fused silica). Various optical elements fabricated using this method have already been demonstrated: fibre Bragg gratings [1], phase masks [2], couplers [3], planar waveguides in various materials [4, 5], devices for biomedical applications [6].

Investigation of the effect of radiation characteristics on the modification parameters (shape, size, refractive index change) is an urgent task. To date, the effect of focusing conditions [7], femtosecond laser writing [8], polarisation [9], energy [10] and wavelength [11] of radiation on the modification parameters has been studied. Temporal characteristics of radiation are additional important factors determining the process of writing, since it is the temporal dynamics of the interaction of various physical processes (multiphoton ionisation, avalanche ionisation, plasma absorption, thermal relaxation) that determine the inscription process. It has been shown that the use of radiation with a high pulse repetition rate (above 1 MHz) to produce waveguide structures makes it possible to obtain higher quality waveguides at a lower pulse energy compared to the case kilohertz repetition rates. This is explained as follows: when the time between pulses is less than the thermal relaxation time ($\sim$1 μs), the accumulation effect comes to the fore, and so subsequent pulses affect the heated area, which requires less energy for modification [12].

Englert et al. [13] presented experimental results for the ablation of fused silica by a femtosecond pulse with an asymmetric temporal shape. The authors used the type of asymmetry that is equivalent to the accumulated chromatic third-order dispersion (TOD). It was shown that for certain values of TOD, it is possible to obtain the modification size that is smaller than the diffraction limit and that is less than the impact of a symmetric pulse. The effect of the pulses is also dependent on the sign of TOD: positive TOD (when first the main pulse arrives) requires less energy per pulse to form the same region as in the case of negative TOD. The reason is that, for the ablation process it is important to reach a certain critical value of the electron density. In the first case (TOD $>$ 0), the main peak produces due to multiphoton ionisation a certain number of electrons, which may be insufficient to reach a critical value, while the secondary peaks (smaller in amplitude) increase the number of electrons due to avalanche ionisation up to a critical value. In the second case (TOD $<$ 0), secondary peaks with a lower amplitude, which is insufficient for multiphoton ionisation, first exert influence. In this case, multiphoton ionisation can only be caused by subsequent (with a larger amplitude) secondary peaks; therefore, only the remaining part of the pulse can produce electrons due to avalanche ionisation. More energy is required in this case, compared to TOD $>$ 0. For this reason, pulses with TOD $>$ 0 are more preferable for the material ablation.

With femtosecond material modification it is also necessary to reach a certain concentration of free electrons, which provide local heating of the material and a subsequent change in its physical properties (e.g., change in the refractive index). Because fabrication of many optical components (waveguides, Bragg gratings) requires action in the bulk of the material, the study of the influence of the temporal pulse shape with TOD $>$ 0, focused into the material, on femtosecond modification is an urgent task.

**A.V. Dostovalov, S.A. Babin** Institute of Automation and Electrometry, Siberian Branch, Russian Academy of Sciences, prosp. Akad. Koptyuga 1, 630090 Novosibirsk, Russia; e-mail: dostovalov@iae.nsk.su;
**A.A. Wolf** Novosibirsk State University, ul. Pirogova 2, 630090 Novosibirsk, Russia;
**M.V. Dubov, V.K. Mezentsev** Aston University, Aston Triangle, Birmingham, B4 7ET, UK

Received 27 July 2012
*Kvantovaya Elektronika* **42** (9) 799–804 (2012)
Translated by I.A. Ulitkin

## 6. Mathematical model

To study numerically propagation of a femtosecond pulse in the material we have selected a model in which plasma is formed in the focusing region due to multiphoton and avalanche ionisation. This model was proposed in [14] and is widely used for such calculations [15]:

$$i\varepsilon_z + \frac{1}{2k}\Delta_\perp\varepsilon - \frac{k''}{2}\frac{\partial^2\varepsilon}{\partial t^2} + k_0 n_2|\varepsilon|^2\varepsilon + \frac{i\sigma}{2}(1+i\omega\tau)\rho\varepsilon + \frac{i\beta^{(K)}}{2}|\varepsilon|^{2(K-1)}\varepsilon = 0, \quad (1)$$

$$\frac{\partial\rho}{\partial\tau} = \frac{1}{n_b^2}\frac{\sigma_{bs}}{E_g}\rho|\varepsilon|^2 + \sigma^{(K)}|\varepsilon|^{2K}, \quad (2)$$

where $k = n_b k_0$ is the wave vector in the medium; $k_0 = \omega/c$; $n_b$ is the refractive index, calculated by the Sellmeier equation [16] for fused silica at 800 nm; $k''$ is the group velocity dispersion; $n_2$ is the nonlinear coefficient describing the Kerr nonlinearity; $\sigma_{bs}$ is the inverse bremsstrahlung cross section; $\tau$ is the electron relaxation time; $E_g$ is the ionisation energy; $\beta(K) = K\hbar\omega\sigma^{(K)}$ is the multiphoton absorption (MPA) coefficient; $K$ is the order of the MPA; $\sigma^{(K)}$ is the parameter characterising multiphoton ionisation.

The wave equation (1) for the complex amplitude $\varepsilon$ of the electric field in the paraxial approximation describes the propagation of a femtosecond pulse in the material along the coordinate $z$ with light diffraction (second term), group velocity dispersion (third term), Kerr nonlinearity (fourth term), avalanche and multiphoton absorption (fifth and sixth terms, respectively) taken into account. Equation (2) for the plasma density $\rho$ contains terms that are responsible for an avalanche ionisation (first term) and multiphoton ionisation (second term).

As an initial condition for equation (1) we used a focused Gaussian beam with a nonzero TOD component. The expression for such a pulse in the frequency domain is given by [17]

$$\varepsilon(z=0,r,\omega) = \varepsilon_0\Delta t\sqrt{\pi/(2\ln 2)} \times \exp\left(-\frac{r^2}{r_0^2} - \frac{ikr^2}{2f} - \frac{\Delta t^2}{8\ln 2}\omega^2 - i\frac{1}{6}\phi_3\omega^3\right), \quad (3)$$

where $\varepsilon_0$ is the initial amplitude of the field; $\Delta t$ is the pulse width (FWHM); $r_0$ is the initial beam radius; $f$ is the focal length of the lens; $\phi_3$ is the TOD parameter, which determines the asymmetry of the beam in time (hereinafter referred to as TOD = $\phi_3/6$). When TOD > 0, a decrease in the modulation amplitude with time is observed (Fig. 1); when TOD < 0, there is an inverse dependence, i.e., an increase in the modulation field amplitude with time.

The calculations were carried out with the following parameters: wavelength, $\lambda = 800$ nm; the order of the MPA, $K = 5$; pulse duration, $\Delta t = 50$ fs; initial beam radius, $r_0 = 2.5$ mm; numerical aperture of the lens, NA = 0.5; ionisation energy, $E_g = 7.6$ eV [18]; group velocity dispersion parameter, $k'' = 361\times10^{-28}$ s$^2$ m$^{-1}$ [18]; nonlinear coefficient, $n_2 = 3.2\times10^{-20}$ W m$^{-2}$ [16]; multiphoton ionisation parameter, $\sigma^{(5)} = 1.3\times10^{-75}$ m$^{10}$ s$^{-1}$ W$^{-5}$ [18]; electron relaxation time, $\tau = 1.7$ fs [19]; critical plasma density, $\rho_{BD} = \varepsilon_0 m_e e^{-2}\omega^2 = 1.74\times10^{27}$ m$^{-3}$. The pulse energy was 115 nJ and TOD varied from $\pm10^6$ fs$^3$ to 0.

## 7. Results of calculations

Figure 1 shows the time dependences of the intensity of asymmetric pulses with TOD = $3\times10^5$, $6\times10^5$ and $1\times10^6$ fs$^3$ at $z = 0$, normalised to the intensity of multiphoton absorption $I_{mpa} = 2.72\times10^{17}$ W m$^{-2}$. The time $t$ is normalised to the value $t_p = \Delta t/\sqrt{2\ln 2}$. The distribution for TOD < 0 has a similar form, but is mirrored around zero. The inset image shows a comparison of the reduced intensity amplitudes with a symmetric pulse amplitude (TOD = 0). One can see that the amplitude of the symmetric pulse is seven times higher than that of the asymmetric pulse, which is caused by the redistribution of the pulse energy to the additional smaller-in-amplitude peaks.

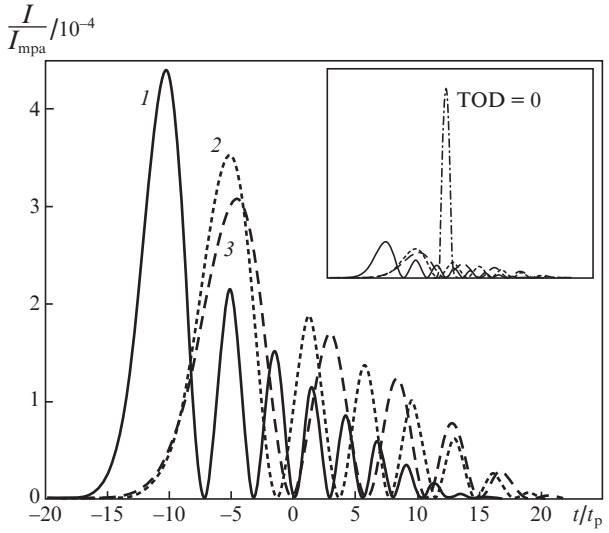


**Figure 1.** Time dependences of the amplitudes of pulse intensities with TOD = $3\times10^5$ (*1*), $6\times10^5$ (*2*) and $1\times10^6$ fs$^3$ (*3*).

Figure 2 shows the dependences of the pulse energy on the propagation coordinate $z$ for different values of TOD and the initial energies of 115 and 200 nJ. As can be seen, the absorbed energy at TOD > 0 is higher than at TOD < 0, which is consistent with the results for the ablation of fused silica [13]. However, the absorbed energy for a symmetric pulse is considerably higher than that of the asymmetric pulse and absorption begins at lower $z$.

At the same time, the data presented in Figure 3 indicate that the density of the plasma generated at the axis ($r = 0$) is maximal both in the case of positive TOD and pulse energy of 115 nJ and in the case of negative TOD and pulse energy of 200 nJ. The time integrated distributions of the density of the generated plasma are shown in Figs 4 and 5 for both cases. The plasma density for the symmetric pulse is localised in a larger volume; therefore, as a result of plasma absorption the pulse is absorbed stronger and the total absorbed energy will be higher.

Figure 6 shows the change in the plasma density with time at $z = 0.181$ mm (at the peak of the plasma density, see Fig. 3). At 115-nJ pulse energy, the plasma density for TOD > 0 is higher than for TOD < 0, which explains the greater absorption of the initial stage of pulse propagation (Fig. 2). One can see that at TOD < 0, the plasma density increases only in the vicinity of zero because of the formation of a plasma under

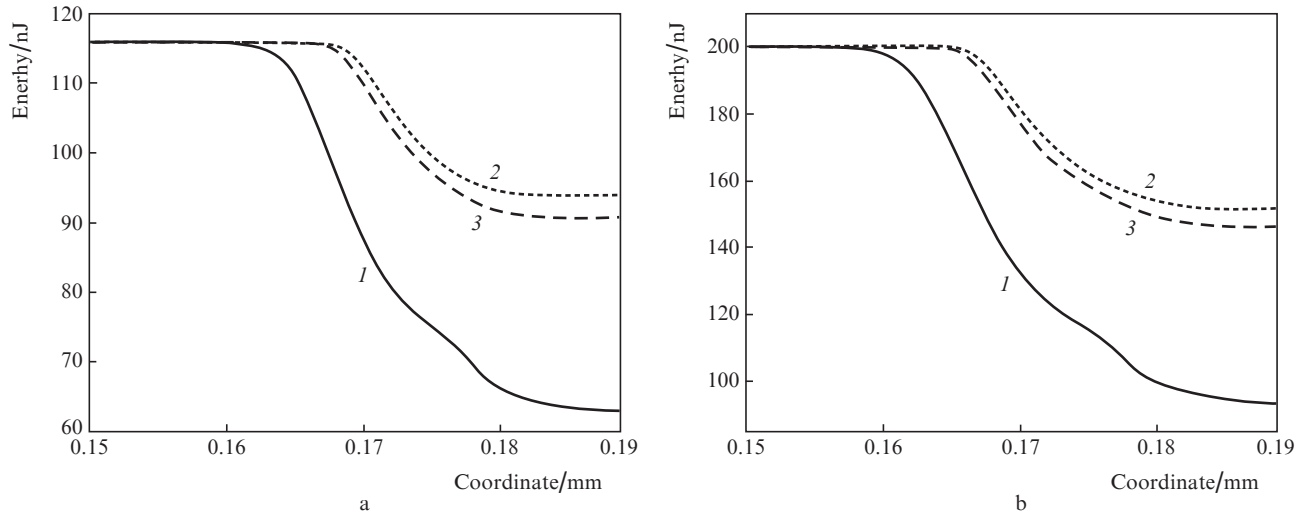


**Figure 2.** Dependences of the pulse energy on the $z$ coordinate for the initial pulse energies 115 (a) and 200 nJ (b) and TOD = 0 (*1*), $-10^6$ (*2*) and $10^6$ fs$^3$ (*3*).

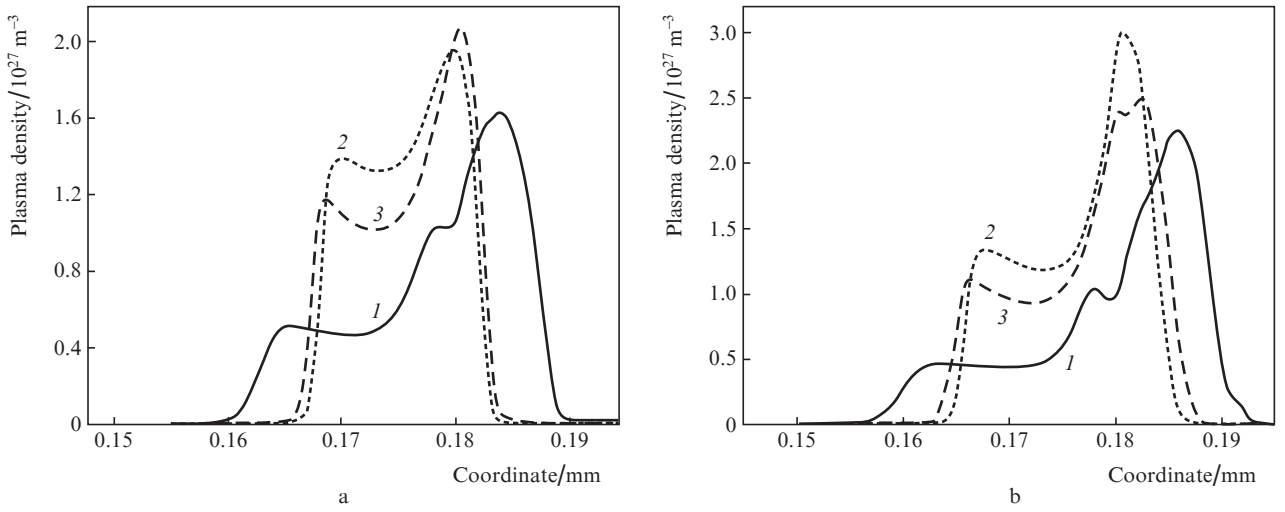


**Figure 3.** Longitudinal distributions of the plasma density on the beam axis ($r = 0$) for the energies 115 (a) and 200 nJ (b) and TOD = 0 (*1*), $-10^6$ (*2*) and $10^6$ fs$^3$ (*3*).

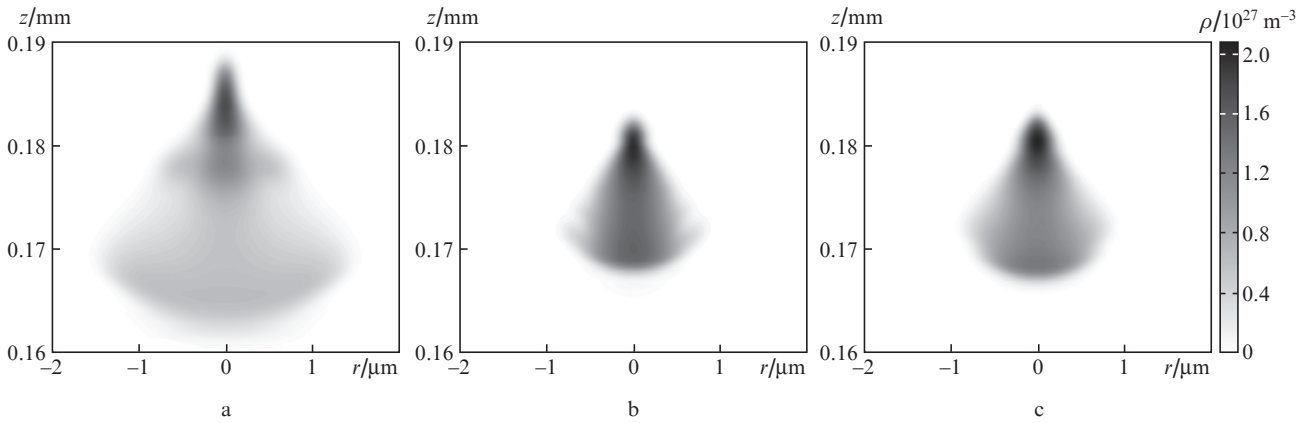


**Figure 4.** Plasma density distribution for the pulse energy 115 nJ and TOD = 0 (a), $-10^6$ (b) and $10^6$ fs$^3$ (c).

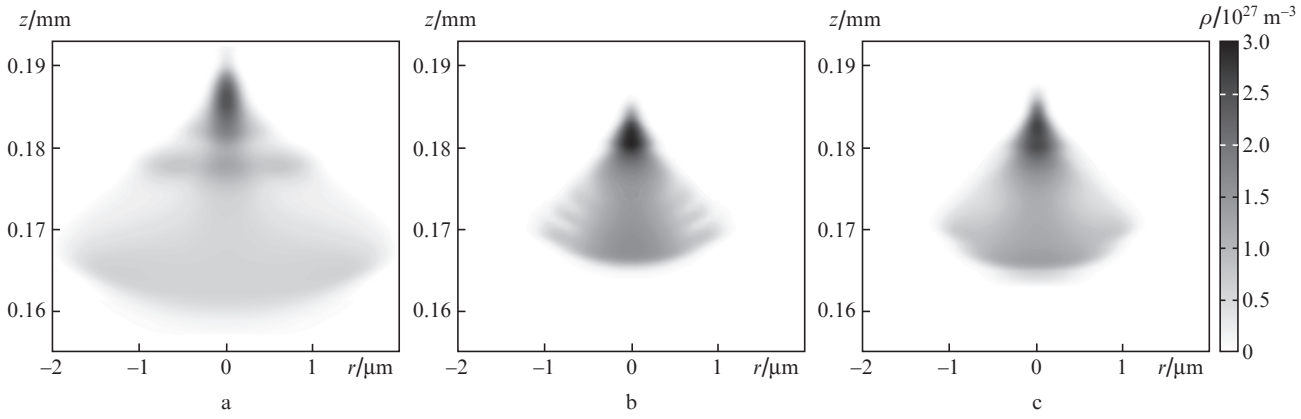


**Figure 5.** Plasma density distribution for the pulse energy 200 nJ and TOD = 0 (a), $-10^6$ (b) and $10^6$ fs$^3$ (c).

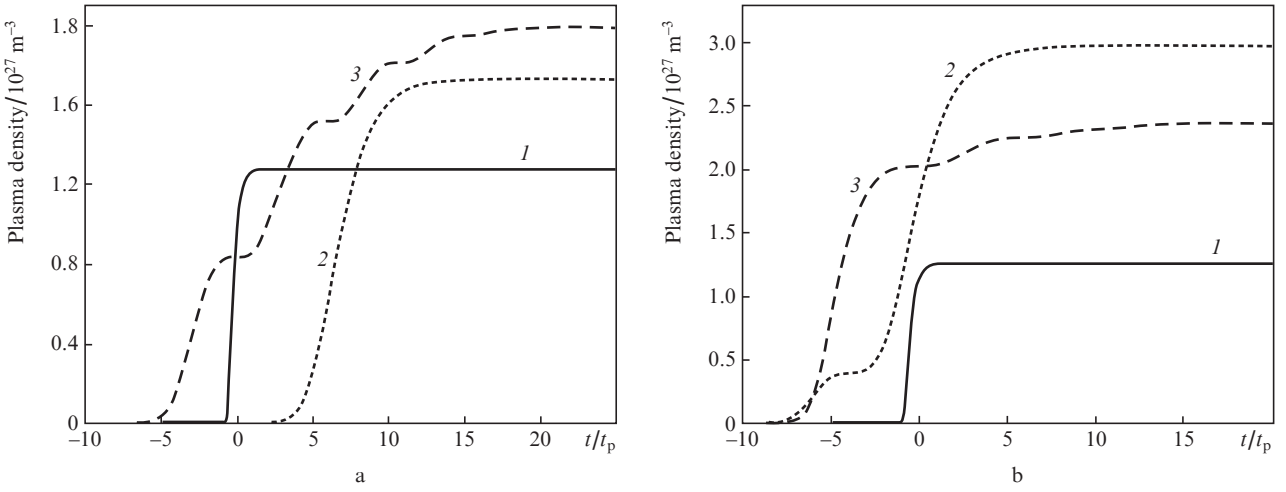


**Figure 6.** Time dependences of the plasma density at $z = 0.181$ mm for TOD = 0 (*1*), $-10^6$ (*2*) and $10^6$ fs$^3$ (*3*) and the initial energy 115 (a) and 200 nJ (b).

the influence of the main peak; in this case, the peaks with a smaller amplitude do not contribute significantly to the generation of plasma. If TOD > 0, the situation is different: after exposure to the peak with a maximum amplitude a certain electron density is generated, which is increased under the action of subsequent smaller-in-amplitude peaks due to avalanche ionisation. Thus, the resulting plasma density in the case of TOD > 0 becomes higher.

However, when the pulse energy is 200 nJ, the maximal plasma density is reached at TOD < 0, which can be explained as follows. With increasing initial energy, the pulse undergoes deformation during propagation (Fig. 7), which depends on the sign of TOD. For TOD > 0 (Fig. 7, left), the pulse experiences deformation in the radial direction because of plasma absorption and defocusing; as a result, the secondary peaks at $r = 0$ almost vanish and do not contribute to the generation of plasma due to avalanche ionisation. At the same time, for TOD < 0 (Fig. 7, right), when secondary peaks with a lower amplitude come to the fore and the effect of the absorption of subsequent peaks is smaller, there remains the effect of secondary peaks and their contribution to the generation of plasma through avalanche ionisation. For this reason, the resulting plasma density is higher in this case.

## 8. Conclusions

We have shown that the use of pulses with TOD ≠ 0 leads to localisation of absorption in the process of femtosecond modification. The density of the plasma generated in this case is higher, which indicates the possibility of obtaining the modification at a lower pulse energy than in the case of a symmetric pulse. In this case, the optimal values of TOD depend on the energy of the pulse. At the initial pulse energy of about 100 nJ, it is preferable to use pulses with TOD > 0. When the energy increases above this value, it is preferable to use pulses with TOD < 0, i.e., at a lower energy the behaviour of the dependence is the same as in the case of ablation of the material, while at a higher energy the effects associated with the propagation of the pulse in the material come to the fore.

## References

1. Martinez A., Dubov M., Khrushchev I., Bennion I. *Electron. Lett.*, **40** (19), 1170 (2004).
2. Smith G.N., Kalli K., Bennion I., Sugden K. *Proc. SPIE Int. Soc. Opt. Eng.*, **7205**, 720511 (2009).
3. Streltsov A.M., Borrelli N.F. *Opt. Lett.*, **26** (1), 42 (2001).
4. Minoshima K., Kowalevicz A.M., Hartl I., Ippen E.P., et al. *Opt. Lett.*, **26** (19), 1516 (2001).

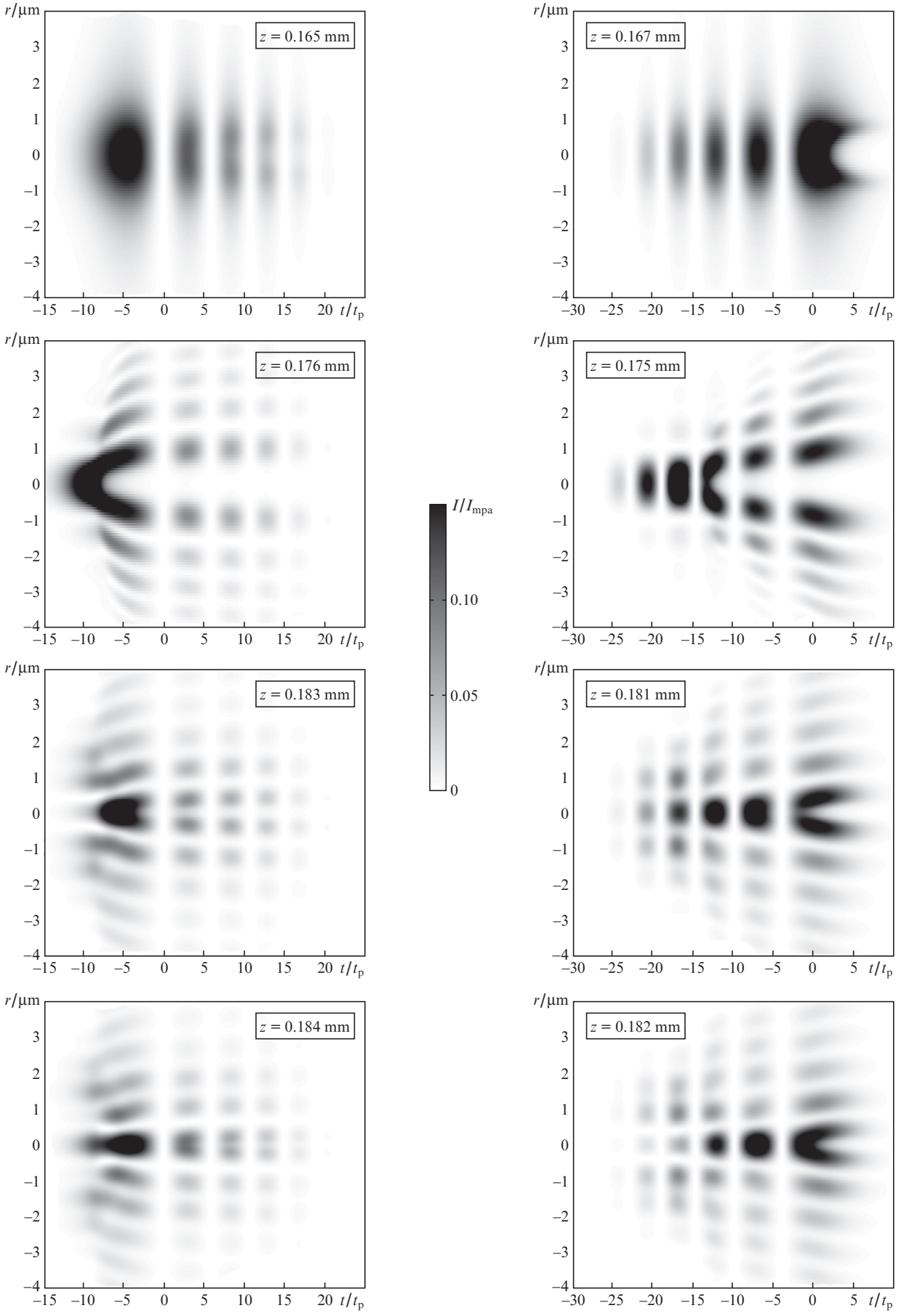


**Figure 7.** Intensity distribution at a 200-nJ pulse energy, different coordinates $z$ and TOD = $10^6$ (left) and $-10^6$ fs$^3$ (right).

5. Kowalevicz A.M., Sharma V., Ippen E.P., Fujimoto J.G., et al. *Opt. Lett.*, **30** (9), 1060 (2005).
6. Schafer D.N., Gibson E.A., Salim E.A., Palmer A.E., et al. *Opt. Express*, **17**, 6068 (2009).
7. Shaffer C., Brouder A., García J., Mazur E. *Opt. Lett.*, **26** (2), 93 (2001).
8. Wong Y., Furniss D., Tikhomirov V.K., Romanova E.A., et al. *Proc. Int. Conf. on Transparent Optical Networks* (Athens, 2008) p. 234.
9. Ams M., Marshall G., Withford M. *Opt. Express*, **14** (26), 13158 (2006).
10. Petrovic J., Schmitz H., Mezentsev V., Bennion I. *Opt. Quantum Electron.*, **39** (10), 939 (2007).
11. Dostovalov A., Babin S., Dubov M., Baregheh M., Mezentsev V. *Laser Phys.*, **5**, 930 (2012).
12. Schaffer C.B., Garcia J.F., Mazur E. *Appl. Phys. A*, **76** (3), 351 (2003).
13. Englert L., Wollenhaupt M., Haag L., Sarpe-Tudoran C., et al. *Appl. Phys. A*, **92** (4), 749 (2008).
14. Feit M., Fleck J. *Appl. Phys. Lett.*, **24** (4), 169 (1974).
15. Sudrie L., Couairon A., Franco M., Lamouroux B. *Phys. Rev. Lett.*, **89**, 186601 (2002).
16. Agrawal D. *Nonlinear Fiber Optics* (CA, San Diego: Academic Press, 2001; Moscow: Mir, 1996).
17. Wollenhaupt M., Assion A., Baumert T. *Handbook of Lasers and Optics* (New York: Springer, 2007).
18. Tzortzakis S., Sudrie L., Franco M., Prade B., et al. *Phys. Rev. Lett.*, **87** (21), 213902 (2001).
19. Mezentsev V., Petrovic J., Dubov M., Bennion I. *Proc. SPIE Int. Soc. Opt. Eng.*, **6459**, 64590B (2007).